HHS Public Access

Author manuscript

*J Orthop Res*. Author manuscript; available in PMC 2019 May 01.

Published in final edited form as:

*J Orthop Res*. 2018 May ; 36(5): 1370–1376. doi:10.1002/jor.23679.

# Muscle Stem Cell Activation in a Mouse Model of Rotator Cuff Injury

**Michael R. Davies**[1,2,†], **Steven Garcia**[3,†], **Stanley Tamaki**[3], **Xuhui Liu**[1,2], **Solomon Lee**[3], **Anthony Jose**[3], **Jason H. Pomerantz**[3], and **Brian T. Feeley**[1,2]

[1]Department of Orthopaedic Surgery, University of California, San Francisco, San Francisco, CA

[2]San Francisco Veterans Affairs Healthcare System, San Francisco, CA

[3]Division of Plastic and Reconstructive Surgery, Departments of Surgery and Orofacial Sciences, Program in Craniofacial Biology, Eli and Edythe Broad Center of Regeneration Medicine, University of California, San Francisco, San Francisco, CA

## Abstract

Rotator cuff (RC) tears are frequently complicated by muscle atrophy. Muscle stem cells (MuSCs) repair damaged myofibers following injury, but their role in the prevention or pathogenesis of atrophy following RC tears remains undefined. We hypothesized that the RC MuSC population would be affected by supraspinatus (SS) and infraspinatus (IS) tendon transection (TT) compared to uninjured muscle in a mouse model of RC tear. C57BL6/J mice underwent unilateral SS and IS TT and contralateral sham surgery. At 3, 8, or 14 weeks after injury, mice were euthanized and SS and IS were harvested for FACS sorting of CD31−/CD45−/Sca1−/ITGa7+/VCAM+ MuSCs or histological analysis. Ki-67+ MuSCs from injured muscle increased 3.4 fold at 3 weeks ($p = 0.03$) and 8.1 fold at 8 weeks ($p = 0.04$) following TT injury, but returned to baseline by 14 weeks ($p = 0.91$). Myod1 remained upregulated 3.3 fold at 3 weeks ($p=0.03$) and 2.0 fold at 14 weeks ($p=0.0003$), respectively. Myofiber cross-sectional area was decreased at both 3 and 14 weeks after injury, but the number of MuSCs per fiber remained relatively constant at 3 ($p=0.3$) and 14 ($p=0.6$) weeks after TT. In this study, we characterized the longitudinal effect of RC tendon injury on the MuSC population in supraspinatus and infraspinatus muscles. MuSCs are transiently activated, and are not depleted, in spite of persistent muscle atrophy.

### Keywords

rotator cuff tears; muscle atrophy; satellite cells; MuSCs; Pax7

*Corresponding Author: Brian T. Feeley, 1500 Owens St., San Francisco, CA 94158, Tel: 415-353-2808, brian.feeley@ucsf.edu.
†These authors contributed equally to this manuscript.

Author Contributions Statement:

MD, SG, XL, JP, BF designed experiments. MD, SG, ST, XL, SL, AJ conducted experiments. Funding provided by grants obtained by BF, XL, and JP. MD, SG, ST, XL, JP, BF wrote, edited, and reviewed manuscript.

## INTRODUCTION

Rotator cuff (RC) tears are among the most common clinically significant musculotendinous injuries, with a prevalence that increases substantially with age[1]. While small and medium-sized tears can be treated surgically with good outcomes, large to massive tears are frequently complicated by failed surgical repair, high re-tear rates, and persistent pain and disability[2]. Muscle atrophy is an independent predictor of poor clinical outcomes following attempted RC repair[3], but the molecular and cellular mechanisms underlying the pathogenesis of muscle atrophy following RC tears remain incompletely understood.

Small animal models of rotator cuff tear involving transection of the supraspinatus and infraspinatus tendons have replicated the pathologic finding of muscle atrophy seen following human RC tears[4–6]. In a previous study, the Akt/mTOR pathway, a known regulator of muscle hypertrophy and muscle stem cell activation[7] was downregulated following tendon transection, suggesting a decrease in protein synthesis following this type of injury[8].

Skeletal muscle stem cells (MuSCs), also known as satellite cells, repair muscle after injury via activation from quiescent states, then migrate, proliferate, and differentiate to repair damaged muscle. The response of MuSCs to RC injury over time, and the role that MuSCs play in the process of muscle atrophy, however, is undefined. Others have previously hypothesized that a decrease in MuSC number, proliferation, or differentiation may contribute to muscle atrophy in chronic injury states[9]. Meyer et al. demonstrated that RC tendon tear state may impact both the population size and proliferative capacity of human skeletal muscle progenitors (SMPs) without hindering their ability to fuse in culture or engraft when transplanted into injured mouse muscle[10]. Thomas et al. likewise demonstrated that human SMPs from injured RC muscle may have impaired proliferative capacity *ex vivo*, but fused into myotubes at higher rates than SMPs from uninjured muscle, suggesting that the local environment of regenerating RC muscle may prime human SMPs for differentiation while limiting their proliferation [11]. In this study, we analyzed the response of murine MuSCs to RC tear over time, correlating their number and activation state with the extent of muscle atrophy observed following RC injury. We hypothesized that RC tear would induce changes in the MuSC population over time, and that understanding these changes would provide insight into RC muscle pathology and the potential of MuSCs as a future therapeutic target to combat muscle atrophy.

## METHODS

### Animal Surgeries

Twenty-four female, twelve-week-old, C57BL/6 mice underwent unilateral supraspinatus (SS) and infraspinatus (IS) tendon transection (TT) with contralateral sham surgery to serve as an internal control, as previously described[4]. All procedures were approved and performed in accordance with the San Francisco Veterans Affairs Healthcare System Institutional Animal Care and Use Committee.

### Muscle Harvest and Cell Sorting

At 3 and 14 weeks after injury, animals were sacrificed (8 animals/time point) and the SS and IS muscles from both the surgery and sham sides were harvested. A subgroup of 8 animals were also sacrificed at 8 weeks to specifically evaluate MuSC midpoint activation state. To obtain sufficient numbers of cells for FACS, the SS and IS muscles from one mouse along with the IS muscle from a second mouse were combined (N = 4/time point) and dissociated into single cells through mechanical mincing and enzymatic digestion with collagenase XI and trypsin, followed with isolation by fluorescence-activated cell sorting (FACS) for the CD31−/CD45−/Sca1−/ITGa7+/VCAM+ MuSC population adapted from the protocol previously described by Liu et al.[12].

### Histological Analysis

Additional representative SS muscles (4 animals/time point/group) were frozen for histological analysis. Previous power analyses revealed that 4 animals/time point/group are sufficient to detect significant differences in muscle weight loss[6] and gene expression[8]. MuSC activation was quantified as follows: MuSCs were sorted by flow cytometry and allowed to seed onto slides for one hour at which time they were washed in PBS and fixed in 4% PFA for 10 minutes followed by immunofluorescent staining with 1:200 rabbit anti-Ki-67 (Thermo) (marker of cell proliferation) and 1:200 mouse anti-Myod1 (BD Biosciences) (marker of myogenic differentiation) of (1) plated sorted MuSCs and (2) whole muscle sections. The number of Ki-67 and Myod1 positive MuSCs in injured muscle was compared to that from the sham-side muscle at 3, 8, and 14 weeks in (1) and at 3 and 14 weeks in (2). In muscle sections, MuSCs were determined to be activated by Pax7 costained with either Ki-67 or Myod1 staining, as reported by Shea et al.[13]. In addition, quantification of the number of MuSCs (Pax7+ cells) per fiber and fiber cross-sectional area (CSA) was performed using ImageJ (NIH). For MuSC counting, all cells in a given cross-sectional image were counted along with all muscle fibers. CSA calculations were performed with circumferential measurements of 100 fibers per muscle section stained with H&E and averaging these measurements to obtain our result.

### Statistical Analysis

Student’s two-tailed t-test was used at each time point between injury and sham group. One-way ANOVA was used to compare multiple time points. For all statistical analyses, data are presented as mean ± standard error.

## RESULTS

### RC Tendon Transection Results in Persistently Decreased Muscle Fiber Size

Fiber CSA in injured muscle was 71.5% ± 1.3 ($p = 0.04$) at 3 weeks after TT injury and 73.6% ± 1.4 ($p = 0.005$) of sham at 14 weeks after injury (Fig. 1), confirming that significant muscle atrophy developed and persisted in this model.

### A Small but Significant Proportion of Isolated MuSCs Enter S-phase in Response to RC Injury Before Returning to Cell Cycle Baseline by 14 Weeks

CD31−/CD45−/Sca1−/ITGa7+/VCAM+ MuSCs were isolated via FACS at 3, 8, and 14 weeks after injury (Fig. 2). Ki-67 staining of purified MuSCs revealed increases in MuSC activation in TT injured muscle at 3 and 8 weeks after injury (3.9% ± 0.6% and 3.3% ± 0.8% respectively), with positive staining ratios of 3.4 ± 0.7 ($p = 0.03$) and 8.1 ± 2.6 ($p = 0.04$) compared to sham (1.1% ± 0.4% and 0.4% ± 0.2%), respectively (Fig. 3). At 14 weeks after injury, there was no significant difference in Ki-67 expression (2.8% ± 0.8%) compared to sham (2.7% ± 0.7%) ($p = 0.91$) (Fig. 3).

### RC Injury Induces Persistent Myod1 Expression in Isolated MuSCs

Myod1 staining of FACS purified MuSCs performed at 3 and 14 weeks after injury demonstrated increases in Myod1 expression in MuSCs from injured muscle (13.8% ± 2.4% and 37.2% ± 1.8%, respectively) compared to sham (4.2% ± 0.8% and 18.9% ± 0.5% respectively), with positive staining ratios of 3.3 ± 0.7 ($p = 0.03$) and 2.0 ± 0.1 ($p = 0.0003$), respectively (Fig. 4).

### MuSCs Return to Baseline Activity and Frequency by 14 Weeks After RC Injury

Quantification of activated MuSCs, defined as Pax7+ cells co-staining with either Ki-67+ or Myod1+ MuSCs in muscle sections, revealed an increase in MuSC activation at 3 weeks after injury (29.2% ± 8.0%) compared to sham (1.9% ± 0.9%), with a positive staining ratio of 15.8 ± 4.6 ($p = 0.04$) (Fig. 5). There was no significant difference in activated MuSCs at 14 weeks after injury (16.0% ± 5.3%) compared to sham (7.0% ± 1.3%) ($p = 0.24$). The ratio of total Pax7+ MuSCs to muscle fiber number was not significantly changed at 3 weeks and 14 weeks post-injury compared to sham ($p = 0.3$ and $p = 0.6$, respectively) (Fig. 5).

## DISCUSSION

In this study, we analyzed the response of MuSCs over time to RC tear in a tendon transection model. We found that while MuSCs undergo an initial increase in activation as evidenced by increased Ki-67 staining *ex vivo* at 3 and 8 weeks identifying an increased proportion of cycling cells. Ki-67 expression returned to baseline by 14 weeks compared to uninjured muscle. Myod1, a marker of MuSC progression from quiescence to activation and differentiation, remains persistently elevated in isolated cells following injury at 14 weeks. Myod1 is a marker of MuSC myogenic commitment, although some Myod1-expressing cells may also serve to replenish the pool of undifferentiated MuSCs rather than progress further down the myogenic lineage[14]. The fact that Myod1 continues to be expressed at later time points compared to Ki-67 in this model is interesting, as prolonged Myod1 expression as a result of epigenetic modifications affecting satellite cell quiescence has been previously associated with eventual depletion of murine MuSCs [15,16].

The number of Pax7+ cells costained with either Ki-67 or Myod1 *in situ* did not significantly differ from that of uninjured muscle by 14 weeks, suggesting that MuSC activation returned to baseline by this later time point. Importantly, we did not observe a decrease in the number of MuSCs per muscle fiber at either 3 or 14 weeks, although we did

observe a persistent decrease in muscle fiber CSA at both of these time points. Together, these findings suggest that there is no intrinsic MuSC depletion in the muscle atrophy observed following RC tears in spite of significantly reduced muscle size. These data suggest atrophic RC muscles retain a full complement of MuSCs, which could participate in recovery of muscle size and function after cuff repair. In the setting of our rotator cuff tear model, strategies that promote activation of MuSCs may be helpful in treating muscle atrophy after tendon repairs.

There may be microenvironmental factors preventing effective muscle repair by MuSCs. In humans, fatty infiltration of rotator cuff muscles is independently linked to poor clinical outcomes[17]. One cellular source of FI and fibrotic tissue that has been recently described is that of fibro/adipogenic progenitor (FAP) cells[18,19]. FAPs increase in response to muscle injury, and may promote early muscle healing via crosstalk with MuSCs[18], but in sustained injury settings such as that of a combined tendon-nerve injury, appear to play a detrimental role to tissue healing via differentiation into pathologic adipocytes and fibroblasts[19,20]. Additionally, increases in extracellular fibrosis have been observed in small animal models of RC tear[21], which may inhibit MuSC function even in spite of an adequate number of cells. Further studies will need to more closely examine the potential crosstalk between the MuSC and FAP populations in order to better determine the relative contributions of each to the prevention and development of muscle atrophy.

This study has certain limitations. First, our model of acute tendon transection does not perfectly replicate the chronic degenerative process of RC tears most commonly seen in humans. Given the chronic nature and extent of muscle retraction frequently observed with human tears, it is widely held that injury of the suprascapular nerve may further contribute to the muscle degeneration seen in human tears, and denervation is frequently a component of small animal models of RC tear. In this study, we were interested in the isolated impact of a massive tendon tear, which was performed acutely. While we typically observe substantial tendon retraction in mice that have undergone this injury at the timepoints that we studied, it is unclear whether this acute mechanical unloading injury has the same chronological impact on muscle stem cells as a chronic tendinous injury. However, numerous studies using this mouse model have shown the development of similar muscle pathology to that seen in human RC tears[4,6,22]. Second, direct functional testing of the MuSC population is necessary in the setting of injury-induced atrophy in order to better assess the capacity of these cells to participate in myotube formation and muscle healing following injury. Specifically, this study denoted cells as “active” if they expressed either the marker of proliferation, Ki67, or the marker of myogenic differentiation, Myod1. However, it was beyond the scope of this study to determine which of these processes individual cells were taking part in, *in situ*. Third, further analysis of additional cell populations involved in the response to RC muscle injury, such as fibro-adpogenic progenitors (FAPs) and inflammatory cells, is necessary for the determination of additional therapeutic targets for improving clinical outcomes in RC tears. Our experimental design could allow for the co-isolation of MuSCs along with other cell types, such as FAPs, in future studies by FACS in muscle subjected to RC tear. Additionally, future work may consider the impact of RC tendon repair on MuSC activation state over time. Finally, the effects of aging on the MuSC population in this animal model

should be considered in future studies, as chronic RC tears in humans are typically seen in the elderly population.

We have shown that SS and IS tendon transection leads to a transient increase in MuSC activity that returns to baseline at an extended time after injury without a decrease in MuSC number in a mouse model of rotator cuff tear. The presence of activated MuSCs does not prevent persistent decreases in myofiber CSA in spite of a maintained MuSC number, suggesting that other factors are primarily responsible for the muscle atrophy seen after RC tears. Together, these data suggest that retained MuSCs in injured rotator cuff muscle after repair may be induced to participate in repair to improve clinical outcomes.

## Acknowledgments

This material is based upon work supported by the U.S. Department of Veterans Affairs, Veterans Health Administration, Office of Research and Development, Biomedical Laboratory Research and Development Merit Review Grant (1I01BX002680), UCSF Core Center for Musculoskeletal Biology and Medicine (NIH 1P30AR066262-01), NIH/NIAMS (RO3 AR060871-02), the Orthopaedic Research and Education Foundation (OREF) Career Development grant, the UCSF Pathways Research Fellowship, the California Institute for Regenerative Medicine (CIRM, RN3-06504), and the UCSF PROF-PATH program (R25MD006832) from the National Institute on Minority Health and Health Disparities.

## References

1. Tempelhof S, Rupp S, Seil R. Age-related prevalence of rotator cuff tears in asymptomatic shoulders. Journal of Shoulder and Elbow Surgery. 1999 Aug 31; 8(4):296–9. [PubMed: 10471998]
2. Galatz LM, Ball CM, Teefey SA, Middleton WD, Yamaguchi K. The outcome and repair integrity of completely arthroscopically repaired large and massive rotator cuff tears. J Bone Joint Surg Am. 2004 Feb 1; 86(2):219–24. [PubMed: 14960664]
3. Gladstone JN, Bishop JY, Lo IK, Flatow EL. Fatty infiltration and atrophy of the rotator cuff do not improve after rotator cuff repair and correlate with poor functional outcome. The American journal of sports medicine. 2007 May 1; 35(5):719–28. [PubMed: 17337727]
4. Liu X, Laron D, Natsuhara K, Manzano G, Kim HT, Feeley BT. A mouse model of massive rotator cuff tears. The Journal of Bone & Joint Surgery. 2012 Apr 4.94(7):e41. [PubMed: 22488625]
5. Rowshan K, Hadley S, Pham K, Caiozzo V, Lee TQ, Gupta R. Development of fatty atrophy after neurologic and rotator cuff injuries in an animal model of rotator cuff pathology. J Bone Joint Surg Am. 2010 Oct 6; 92(13):2270–8. [PubMed: 20926720]
6. Liu X, Manzano G, Kim HT, Feeley BT. A rat model of massive rotator cuff tears. Journal of orthopaedic research. 2011 Apr 1; 29(4):588–95. [PubMed: 20949443]
7. Han B, Tong J, Zhu MJ, Ma C, Du M. Insulin-like growth factor-1 (IGF-1) and leucine activate pig myogenic satellite cells through mammalian target of rapamycin (mTOR) pathway. Molecular reproduction and development. 2008 May 1; 75(5):810–7. [PubMed: 18033679]
8. Liu X, Joshi SK, Samagh SP, Dang YX, Laron D, Lovett DH, Bodine SC, Kim HT, Feeley BT. Evaluation of Akt/mTOR activity in muscle atrophy after rotator cuff tears in a rat model. Journal of Orthopaedic Research. 2012 Sep 1; 30(9):1440–6. [PubMed: 22378614]
9. Jejurikar SS, Kuzon WM Jr. Satellite cell depletion in degenerative skeletal muscle. Apoptosis. 2003 Dec 1; 8(6):573–8. [PubMed: 14574063]
10. Meyer GA, Farris AL, Sato E, Gibbons M, Lane JG, Ward SR, Engler AJ. Muscle progenitor cell regenerative capacity in the torn rotator cuff. Journal of Orthopaedic Research. 2015 Mar 1; 33(3): 421–9. [PubMed: 25410765]
11. Thomas KA, Gibbons MC, Lane JG, Singh A, Ward SR, Engler AJ. Rotator cuff tear state modulates self-renewal and differentiation capacity of human skeletal muscle progenitor cells. Journal of Orthopaedic Research. 2016 Oct 1.

12. Liu L, Cheung TH, Charville GW, Rando TA. Isolation of skeletal muscle stem cells by fluorescence-activated cell sorting. Nature protocols. 2015 Oct 1; 10(10):1612–24. [PubMed: 26401916]

13. Shea KL, Xiang W, LaPorta VS, Licht JD, Keller C, Basson MA, Brack AS. Sprouty1 regulates reversible quiescence of a self-renewing adult muscle stem cell pool during regeneration. Cell stem cell. 2010 Feb 5; 6(2):117–29. [PubMed: 20144785]

14. Dhawan J, Rando TA. Stem cells in postnatal myogenesis: molecular mechanisms of satellite cell quiescence, activation and replenishment. Trends in cell biology. 2005 Dec 31; 15(12):666–73. [PubMed: 16243526]

15. Boonsanay V, Zhang T, Georgieva A, Kostin S, Qi H, Yuan X, Zhou Y, Braun T. Regulation of Skeletal Muscle Stem Cell Quiescence by Suv4-20h1-Dependent Facultative Heterochromatin Formation. Cell stem cell. 2016 Feb 4; 18(2):229–42. [PubMed: 26669898]

16. Jiang C, Wen Y, Kuroda K, Hannon K, Rudnicki MA, Kuang S. Notch signaling deficiency underlies age-dependent depletion of satellite cells in muscular dystrophy. Disease Models and Mechanisms. 2014 Aug 1; 7(8):997–1004. [PubMed: 24906372]

17. Barry JJ, Lansdown DA, Cheung S, Feeley BT, Ma CB. The relationship between tear severity, fatty infiltration, and muscle atrophy in the supraspinatus. Journal of Shoulder and Elbow Surgery. 2013 Jan 31; 22(1):18–25. [PubMed: 22541866]

18. Joe AW, Yi L, Natarajan A, Le Grand F, So L, Wang J, Rudnicki MA, Rossi FM. Muscle injury activates resident fibro/adipogenic progenitors that facilitate myogenesis. Nature cell biology. 2010 Feb 1; 12(2):153–63. [PubMed: 20081841]

19. Liu X, Ning AY, Chang NC, Kim H, Nissenson R, Wang L, Feeley BT. Investigating the cellular origin of rotator cuff muscle fatty infiltration and fibrosis after injury. Muscles, Ligaments and Tendons Journal. 2016 Jan.6(1):6.

20. Fiore D, Judson RN, Low M, Lee S, Zhang E, Hopkins C, Xu P, Lenzi A, Rossi FM, Lemos DR. Pharmacological blockage of fibro/adipogenic progenitor expansion and suppression of regenerative fibrogenesis is associated with impaired skeletal muscle regeneration. Stem Cell Research. 2016 Jul 31; 17(1):161–9. [PubMed: 27376715]

21. Sato EJ, Killian ML, Choi AJ, Lin E, Esparza MC, Galatz LM, Thomopoulos S, Ward SR. Skeletal muscle fibrosis and stiffness increase after rotator cuff tendon injury and neuromuscular compromise in a rat model. Journal of Orthopaedic Research. 2014 Sep 1; 32(9):1111–6. [PubMed: 24838823]

22. Deprés-tremblay G, Chevrier A, Snow M, Hurtig MB, Rodeo S, Buschmann MD. Rotator cuff repair: a review of surgical techniques, animal models, and new technologies under development. Journal of Shoulder and Elbow Surgery. 2016 Aug 20.

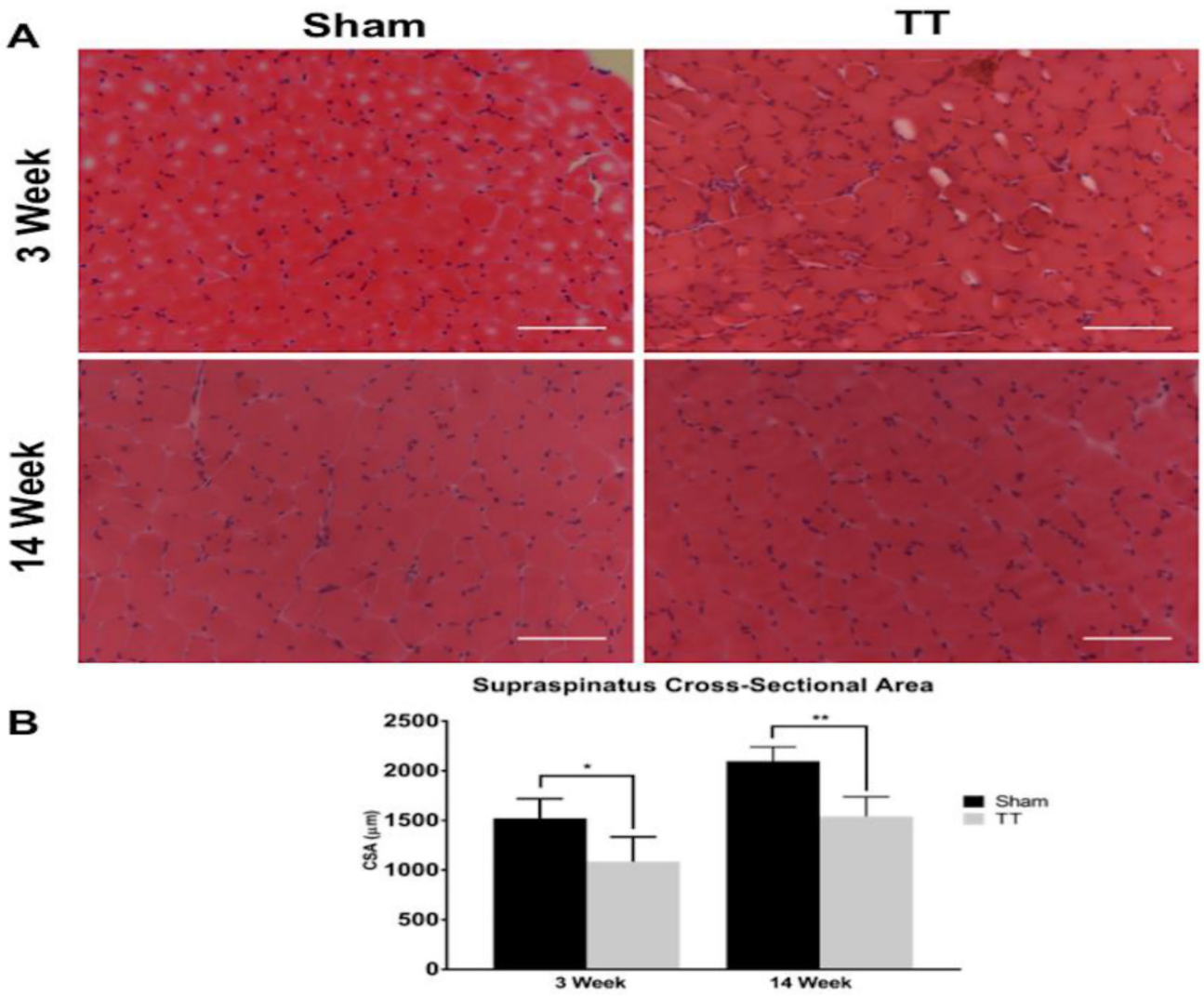


**Fig. 1. Characterization of muscle fiber cross-sectional area after tendon transection**

(A) Representative H&E sections from sham and TT injured supraspinatus muscles showing decreased myofiber size in TT muscles compared to sham at 3 and 14 weeks post injury. Left panels depict representative sham SS sections at 3 and 14 weeks. Right panels depict representative TT injured SS sections at 3 and 14 weeks. Scale bar represents 100μm.

(B) Quantification of myofiber cross-sectional area in sham and TT injured supraspinatus muscles showing significantly decreased myofiber size in TT muscles compared to sham at 3 and 14 weeks post injury. N = 4 for each condition depicted. * $p < 0.05$, ** $p < 0.005$.

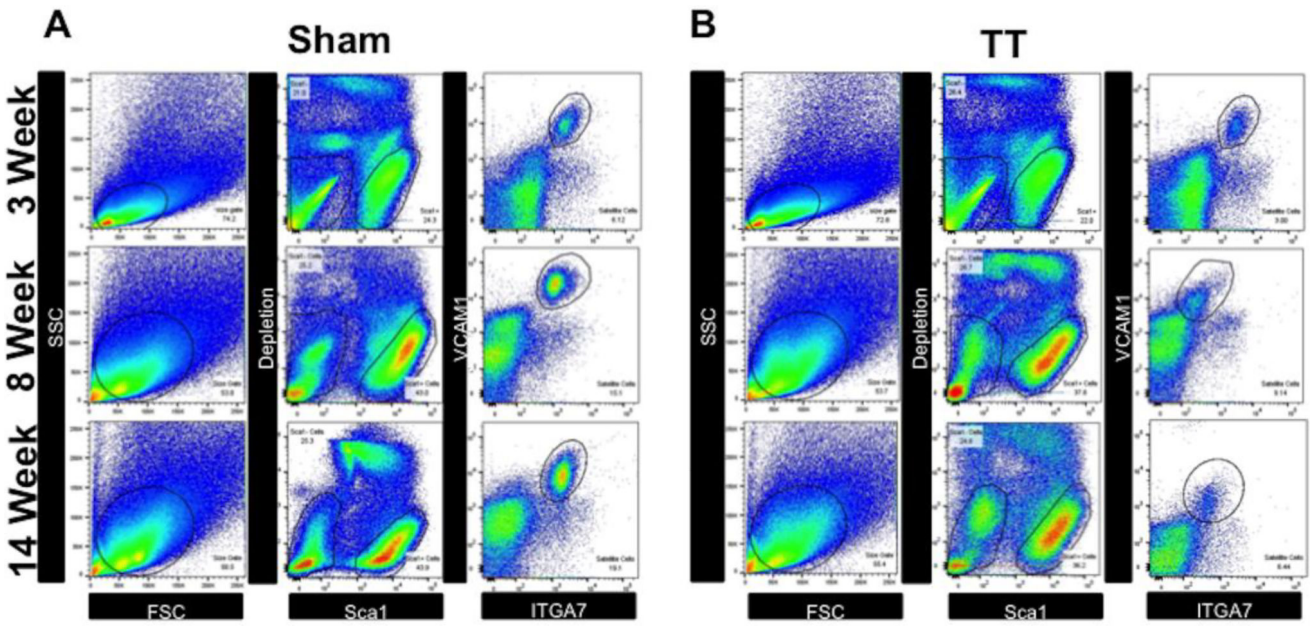


**Fig. 2. Fluorescence-activated cell sorting of MuSCs from RC muscle**

(A–B) Whole RC muscle was digested into single cell suspensions and stained with anti-CD31, anti-CD45, anti-Sca1, anti-ITGA7, and anti-VCAM1 antibodies. Stained cell suspensions were then then sorted by the following schema: SSC/FSC granularity/size gating (left panels), removal of doublets (no shown), followed by depletion of CD31, CD45, Sca1 cells, and sytox positive cells (middle panels), and finally positive selection and sorting of ITGA7/VCAM1 double positive MuSCs (right panels).

(A) Representative FACS sorting gates from sham muscle at 3 weeks, 8 weeks, and 14 weeks.

(B) Representative FACS sorting gates from TT injured muscle at 3 weeks, 8 weeks, and 14 weeks.

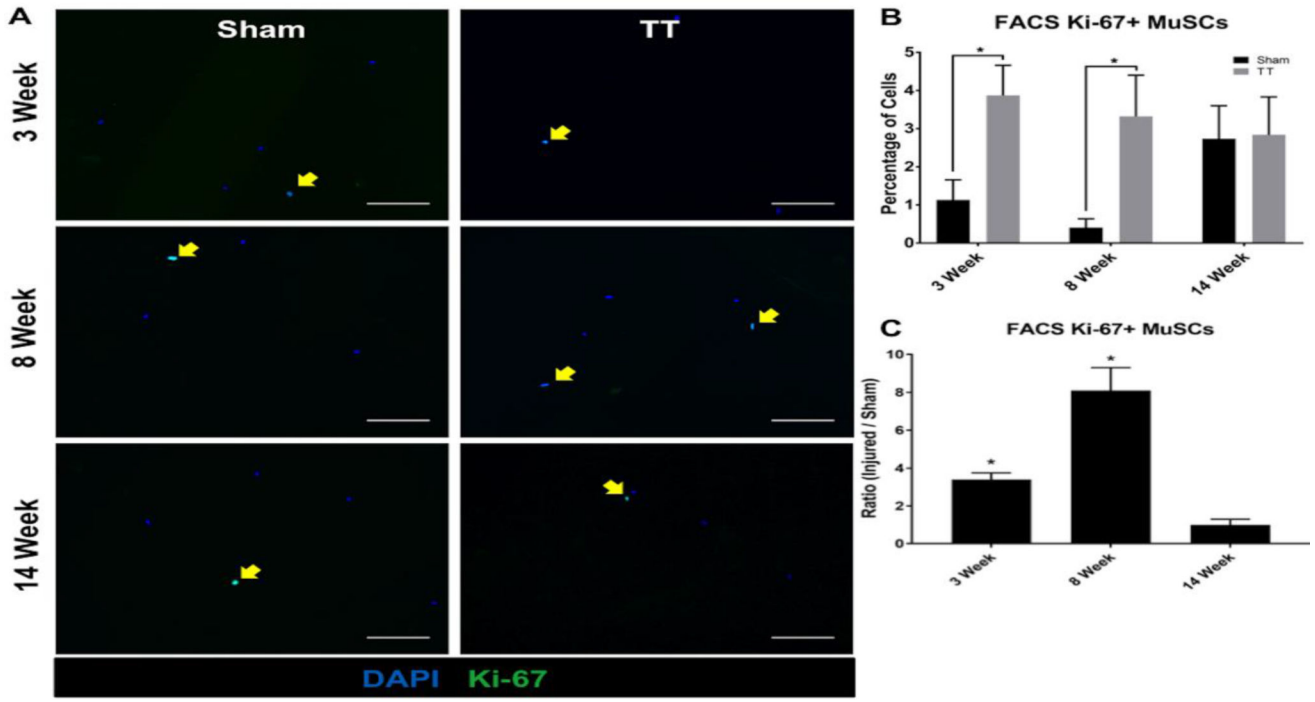


**Fig. 3. Quantification of Ki-67 positive MuSCs sorted from RC muscle**

(A) Representative immunofluorescence images of MuSCs isolated from sham and TT injured RC muscle at 3 weeks, 8 weeks, and 14 weeks post-surgery stained with DAPI (blue) and anti-Ki-67 antibody (green). Left panels depict MuSCs from sham RC muscle. Right panels depict MuSCs from TT injured RC muscle. Ki-67 positive MuSCs are indicated by yellow arrows. Scale bars represent 100μm.

(B) Bar graph showing the percentage of Ki-67 positive live cells sorted in both TT injured and sham groups at 3, 8, and 14 weeks. N = 4 were analyzed for each condition depicted. * $p < 0.05$.

(C) Bar graph showing the ratio of Ki-67 positive MuSCs in TT injured versus sham groups. N = 4 were analyzed for each condition depicted. * $p < 0.05$.

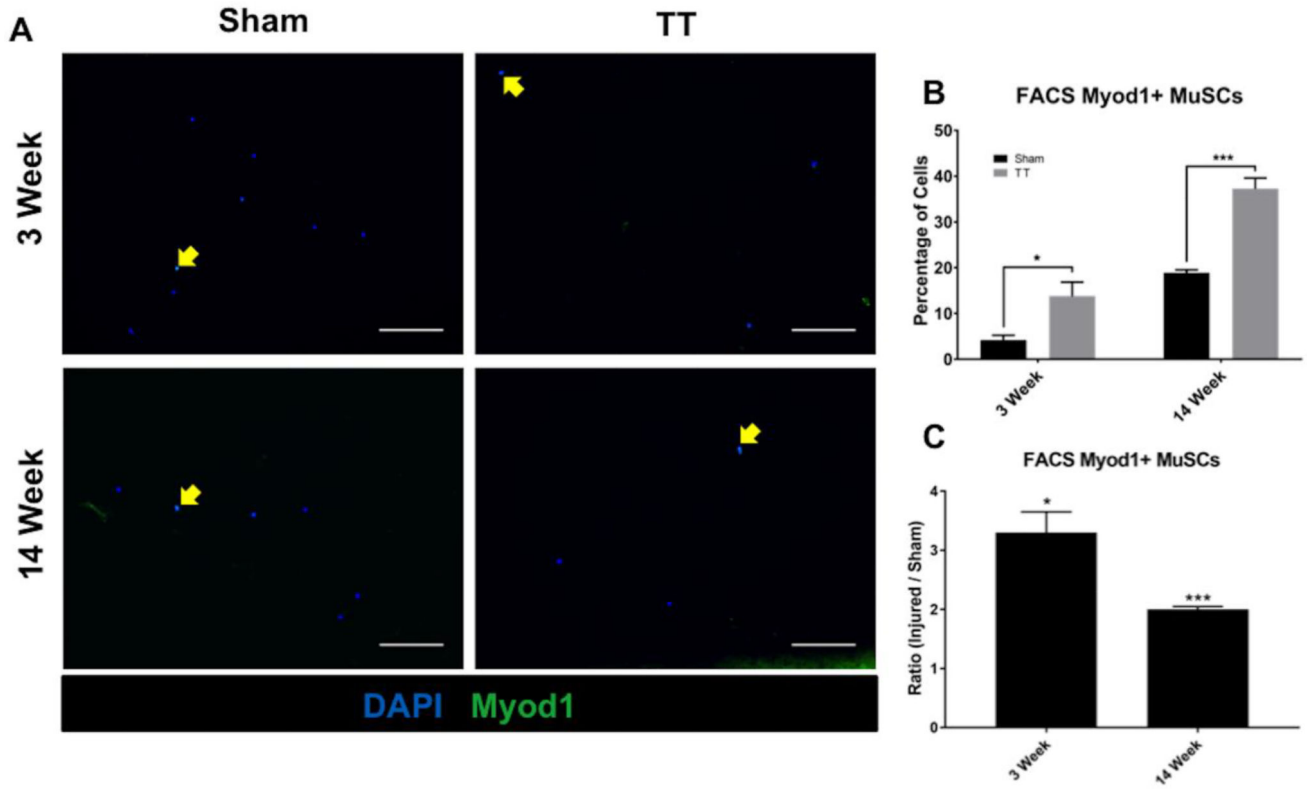


**Fig. 4. Quantification of Myod1 positive MuSCs sorted from RC muscle**

(A) Representative immunofluorescence images of MuSCs isolated from sham and TT injured RC muscle at 3 weeks and 14 weeks post-surgery stained with DAPI (blue) and anti-Myod1 antibody (green). Left panels depict MuSCs from sham RC muscle. Right panels depict MuSCs from TT injured RC muscle. Myod1 positive MuSCs are indicated by yellow arrows. Scale bars represent 100μm.

B) Bar graph showing the percentage of Myod1 positive live cells sorted in both TT injured and sham groups. N = 4 were analyzed for each condition depicted. * $p < 0.05$, ***<0.0005.

(C) Bar graph showing the ratio of Myod1 positive MuSCs in TT injured versus sham experimental groups. N = 4 were analyzed for each condition depicted. * $p < 0.05$, *** $p < 0.0005$.

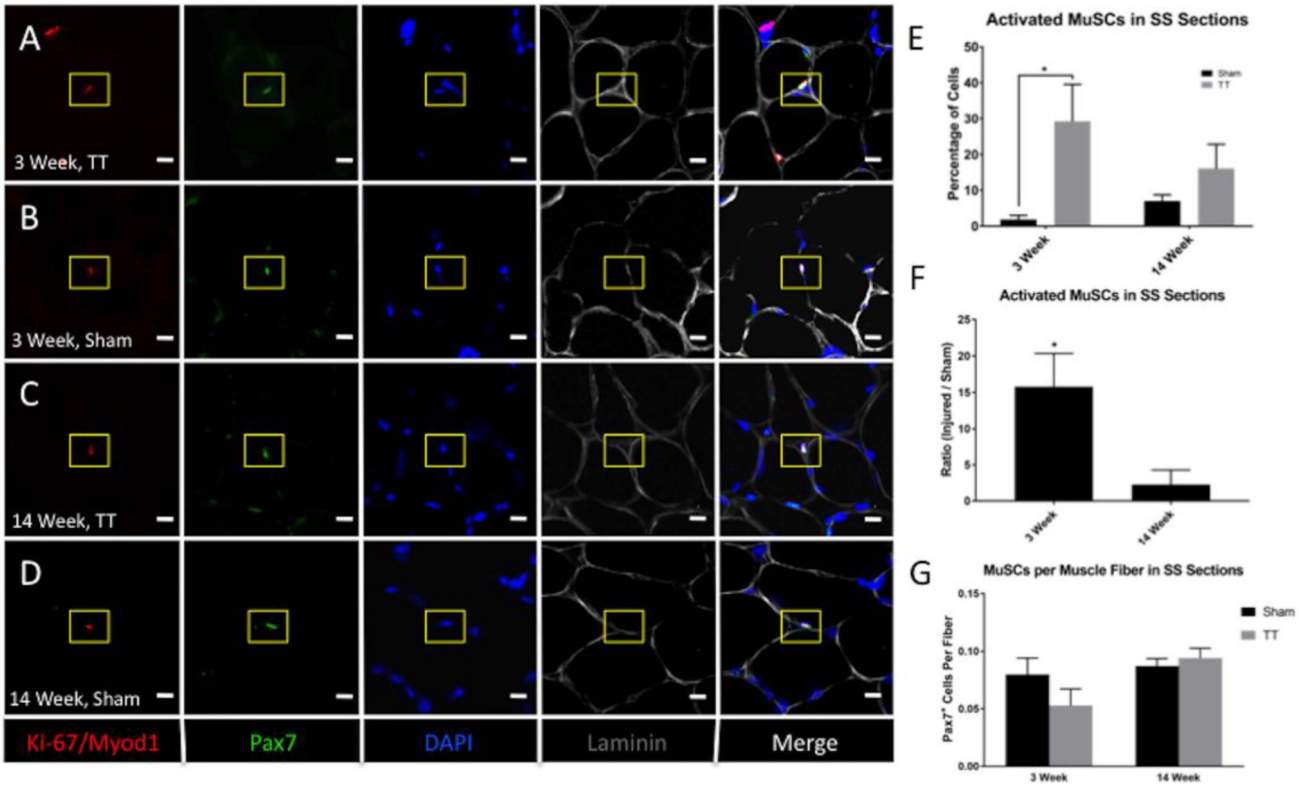


**Fig. 5. In situ characterization of MuSCs after tendon transection**

(A–D) Representative immunofluorescence images of SS muscle sections from TT injured and sham muscle a 3 weeks and 14 weeks post-surgery. Sections were stained with anti-Pax7 (green), anti-Myod1 and anti-Ki-67 (red), laminin (grey), and DAPI (blue). Rows A and C depict images of TT injured SS muscle. Rows B and D depict images from sham SS muscle. Ki-67/Myod1 and Pax7 double positive MuSCs are indicated by yellow boxes. Scale bar represents 10μm.

(E) Bar graph quantifying the percentage of active MuSCs in TT injured compared to sham experimental groups. N = 4 were analyzed for each condition depicted. * $p < 0.05$.

(F) Bar graph quantifying the ratio of MuSCs in TT injured versus sham experimental groups. N = 4 were analyzed for each condition depicted. * $p < 0.05$.

(G) Bar graph quantifying the number of MuSCs per muscle fiber in TT injured and sham experimental groups. N = 4 were analyzed for each condition depicted. * $p < 0.05$.